Specific T-type calcium channel isoforms are associated with distinct burst phenotypes in deep cerebellar nuclear neurons

Michael L. Molineux*, John E. McRory*, Bruce E. McKay*, Jawed Hamid*, W. Hamish Mehaffey*, Renata Rehak*, Terrance P. Snutch†, Gerald W. Zamponi*, and Ray W. Turner*‡

*Hotchkiss Brain Institute, University of Calgary, Calgary, AB, Canada T2N 4N1; and †Michael Smith Laboratories, University of British Columbia, Vancouver, BC, Canada V6T 1Z4

T-type calcium channels are thought to transform neuronal output to a burst mode by generating low voltage-activated (LVA) calcium currents and rebound burst discharge. In this study we assess the expression pattern of the three different T-type channel isoforms ($Ca_v3.1$, $Ca_v3.2$, and $Ca_v3.3$) in cerebellar neurons and focus on their potential role in generating LVA spikes and rebound discharge in deep cerebellar nuclear (DCN) neurons. We detected expression of one or more Ca_v3 channel isoforms in a wide range of cerebellar neurons and selective expression of different isoforms in DCN cells. We further identify two classes of large-diameter DCN neurons that exhibit either a strong or weak capability for rebound discharge, despite the ability to generate LVA spikes when calcium currents are pharmacologically isolated. By correlating the Ca_v3 channel expression pattern with the electrophysiological profile of identified DCN cells, we show that $Ca_v3.1$ channels are expressed in isolation in DCN-burst cells, whereas $Ca_v3.3$ is expressed in DCN-weak burst cells. $Ca_v3.1$-expressing DCN cells correspond to excitatory or GABAergic neurons, whereas $Ca_v3.3$-expressing cells are non-GABAergic. The Ca_v3 class of LVA calcium channels is thus expressed in specific combinations in a wide range of cerebellar neurons but contributes to rebound burst discharge in only a select number of cell classes.

Purkinje cells | cerebellum | rebound discharge

Low voltage-activated (LVA) calcium channels typically activate near −60 mV and display rapid inactivation at depolarized membrane potentials, although their properties can vary considerably depending on the neuronal cell type (1). Molecular analyses have identified three T-type calcium channel isoforms ($\alpha_{1G}/Ca_v3.1$, $\alpha_{1H}/Ca_v3.2$, and $\alpha_{1I}/Ca_v3.3$) that display distinct kinetic properties in heterologous expression systems (2–5). The variability of T-type currents observed in neurons may then reflect a differential expression pattern of Ca_v3 channel isoforms.

At resting membrane potentials T-type channels are typically inactivated and therefore contribute little to spike generation. A brief hyperpolarization promotes recovery of T-type channels, and upon release from the hyperpolarizing influence they depolarize the membrane to generate a LVA calcium spike and rebound depolarization that drives a burst of Na^+ spikes (6–9). Rebound bursts have been shown to modify the output of different cerebellar neurons. In particular, deep cerebellar nuclear (DCN) neurons generate rebound bursts in response to Purkinje cell inhibitory input (10–13), a response that has been proposed to contribute to a reverberating timing loop important for cerebellar functions (14). In Purkinje cells T-type calcium channels contribute to both the burst and interburst depolarizations, indicating roles beyond strictly bursting (15). In situ hybridization studies report $Ca_v3.1$ mRNA in at least DCN and Purkinje cells (16, 17). However, reports of rebound burst discharge in other cerebellar cell types would suggest that Ca_v3 calcium isoforms may be more widely expressed than realized (18–20), with the potential for T-type channel isoforms to differentially contribute to cerebellar neuronal output.

In the present study we determined the distribution of $Ca_v3.1$, $Ca_v3.2$, and $Ca_v3.3$ T-type channel isoforms in cerebellar cell types and their role in generating rebound burst discharge. The results show that Ca_v3 channel isoforms are expressed in all major cerebellar cell types, and that more than one isoform can be coexpressed per cell class. We find that selective expression of $Ca_v3.1$ channels is sufficient to support rebound discharge in one DCN cell class, whereas a contribution by $Ca_v3.3$ to rebound discharge in a different class of DCN cells is constrained by coexpression of potassium channels.

Results

Distinct Distributions of Ca_v3 T-Type Calcium Channel Isoforms. We determined the expression pattern of $Ca_v3.1$, $Ca_v3.2$, and $Ca_v3.3$ channel isoforms by using polyclonal antibodies directed against unique regions of Ca_v3 channel α_1 subunits (see Fig. 7, which is published as supporting information on the PNAS web site). Expression of Ca_v3 channel immunolabel was assessed for the prominent cell types in cerebellum, including Purkinje cells, DCN neurons, granule cells, Golgi cells, stellate cells, and basket cells. In general, virtually all neuronal cell types expressed one or more of the Ca_v3 channel isoforms, often with specific subcellular distributions. Ca_v3 immunolabel was localized primarily to neuronal somata or processes in some cell types and as either a uniform label that could delineate the boundaries of a soma or process or as punctate membrane-associated staining.

Purkinje cells provided some of the most distinctive labels in terms of T-type calcium channel distributions (Fig. 1 A–C). $Ca_v3.1$ immunolabel in Purkinje cells was essentially restricted to the cell body region, with only a few examples of dendritic label across multiple sections (Fig. 1A). $Ca_v3.2$ immunolabel was generally weak and found predominantly at Purkinje cell somata or in rare cases Purkinje cell dendrites (Fig. 1B). By comparison, strong immunolabel for $Ca_v3.3$ was found in the cell body and extensive regions of the dendritic arbor (Fig. 1C). Cells of the DCN are heterogeneous in being composed of both excitatory and inhibitory cell classes that include neurons with small-diameter (<20 μm) to large-diameter (>20 μm) cell bodies (21–23). Ca_v3 immunolabel in the DCN neurons differed from cortical regions as it exhibited a diffuse interstitial label within the boundaries of the nuclei; a label that was entirely absent when Ca_v3 antibodies were omitted or preabsorbed with purified protein (see Fig. 7). The source of the diffuse label was not strictly identified, but likely reflects the extremely dense network of small-diameter axonal, dendritic, and glial processes in the
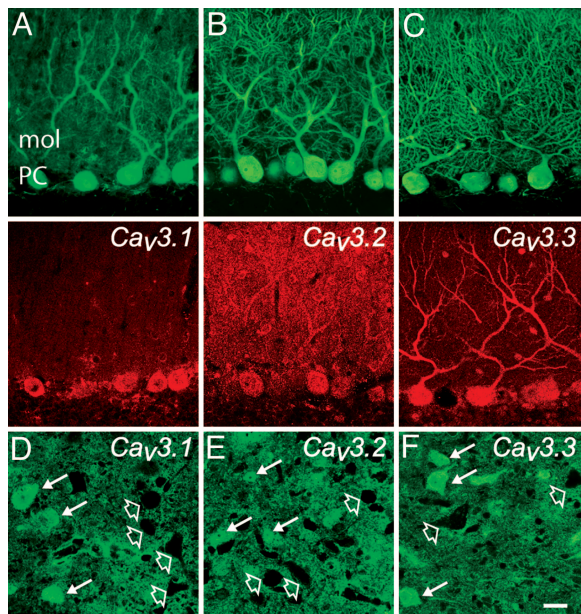

NEUROSCIENCE

Fig. 1. Ca$_v$3.1, Ca$_v$3.2, and Ca$_v$3.3 immunolabel of cerebellar output neurons. (*A–C*) Images of cerebellar Purkinje cells double-labeled for calbindin are paired with images of Ca$_v$3 immunolabel. mol, molecular; PC, Purkinje cell. (*D–F*) Ca$_v$3.1, Ca$_v$3.2, and Ca$_v$3.3 labeling of DCN neurons. A diffuse interstitial label allows one to distinguish a heterogeneous Ca$_v$3 expression pattern in DCN neurons. Filled arrows indicate Ca$_v$3-positive neurons and open arrows indicate DCN neurons negative for a given Ca$_v$3 immunolabel. (Scale bar: 20 μm.)

DCN neurons. This diffuse label proved helpful in identifying distinct populations of DCN neurons that were clearly negative or positive for Ca$_v$3 immunolabel (Fig. 1 *D–F*). Ca$_v$3.1 immunolabel was restricted to the somata of a class of large-diameter DCN neurons and completely absent from neighboring large- and small-diameter neurons (Fig. 1*D*). In contrast, Ca$_v$3.2 label was found predominantly on small-diameter DCN cells and on occasion larger-diameter neurons (Fig. 1*E*). Ca$_v$3.3 immunolabel was constrained to somata and at least proximal dendrites of a set of large-diameter DCN neurons, again leaving another group of large and small neurons unlabeled (Fig. 1*F*).

Specific Ca$_v$3 expression patterns were apparent in cerebellar cortical interneurons (Fig. 2). Golgi cells proved to be unique among interneurons examined here in expressing only the Ca$_v$3.1 channel subtype (Fig. 2*A*) with no label for Ca$_v$3.2 or Ca$_v$3.3 (Fig. 2 *D* and *G*). Stellate cells were negative for Ca$_v$3.1, but positive for Ca$_v$3.2 and Ca$_v$3.3 (Fig. 2 *B*, *E*, and *H*). Basket cells exhibited Ca$_v$3 channel immunolabel at much lower intensity than stellate cells and were heterogeneous in being either positive or negative for immunolabel. Basket cells were thus negative for Ca$_v$3.1 immunolabel (Fig. 2*C*) and were routinely, but not always, positive for Ca$_v$3.2 or Ca$_v$3.3 (Fig. 2 *F* and *I*). The reported expression pattern of Ca$_v$3 isoforms and the ability to record T-type currents in granule cells has been variable and linked to the developmental stage (16, 24). We found no consistent pattern of immunolabel for Ca$_v$3.1 in granule cells in sagittal or coronal planes, only faint immunolabel for Ca$_v$3.2, and an inconsistent immunolabel for Ca$_v$3.3 (data not shown).

In summary, our data show that individual Ca$_v$3 isoforms can be expressed either alone or in combination with other Ca$_v$3 isoforms in cerebellar cells. Immunolabel is also evident in a greater range of cell classes than expected based on previous *in situ* hybridization work (16, 17). To determine the functional significance of these distributions, we used electrophysiology to test for potential T-type-mediated responses.
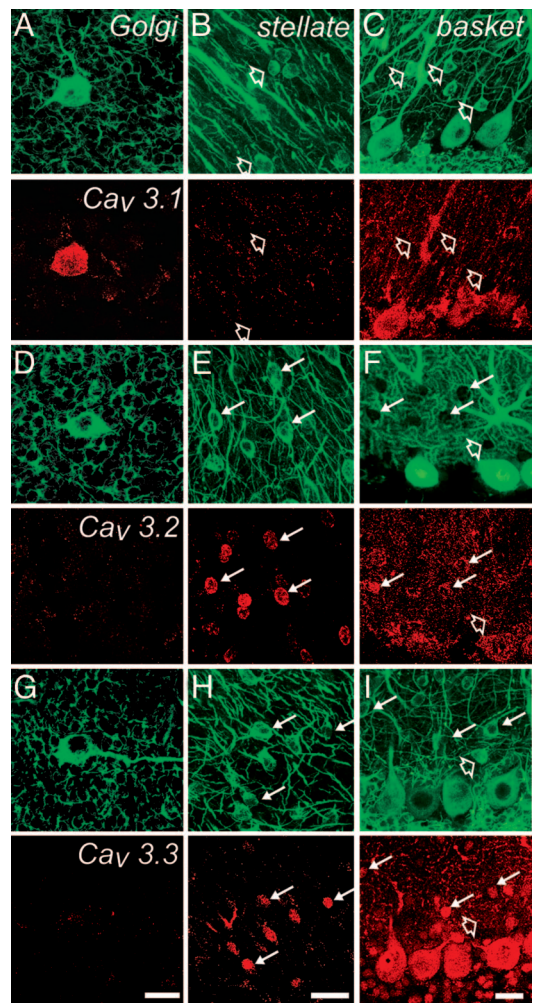

Fig. 2. Ca$_v$3 isoform expression in cerebellar interneurons. Cerebellar interneuron image pairs of Ca$_v$3.1, Ca$_v$3.2, or Ca$_v$3.3 immunolabel are shown juxtaposed to microtubule-associated protein-2-labeled cell bodies and dendrites. Labeling of Golgi cells (*A*, *D*, and *G*), stellate cells (*B*, *E*, and *H*), and basket cells (*C*, *F*, and *I*) is shown. The structural immunolabel in *F* is calbindin, revealing basket cells as negative images against a background of Purkinje cell dendrites. Filled arrows denote cells positive for immunolabel, and open arrows indicate those negative for Ca$_v$3 immunolabel. (Scale bars: 20 μm.)

Ca$_v$3-Expressing Cells Exhibit Variable Degrees of Rebound Burst Discharge. The classic electrophysiological signature for T-type channel expression is the generation of a rebound depolarization and spike burst after a membrane hyperpolarization. We thus obtained whole-cell patch recordings from key cell types exhibiting Ca$_v$3 immunolabel to examine their capacity to generate rebound bursts. We were particularly interested in the rebound burst capabilities of DCN cells given the known propensity of these cells to generate bursts (25, 26). Moreover, DCN cells exhibited a very specific expression pattern for Ca$_v$3 channels in being strongly positive or negative for a particular isoform (Fig. 1 *D–F*), leading to the potential for a specific isoform to be associated with a given firing pattern. We restricted recordings to large-diameter cells as they can include both excitatory and inhibitory neurons (21). We further contrasted the activity of DCN cells to that of Purkinje cells, which express all three Ca$_v$3 isoforms, and Golgi cells that express only Ca$_v$3.1.

To test rebound burst capability we constructed frequency-current (FI) plots from two series of test pulses with and without a preceding hyperpolarization (Fig. 3). The first set of test pulses was
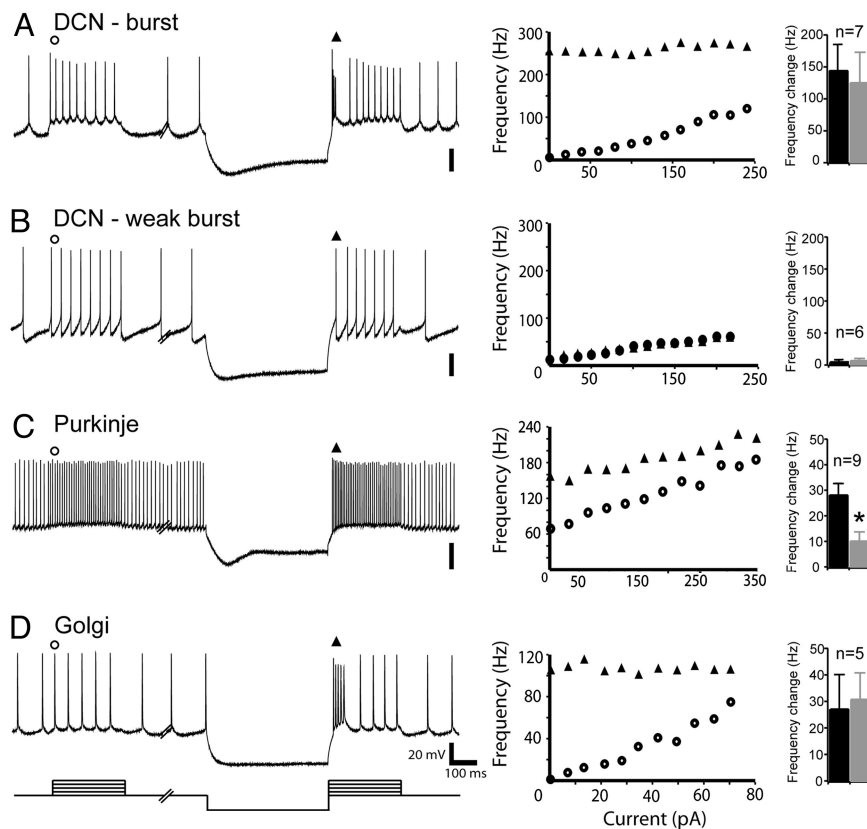
Fig. 3. Cerebellar cells exhibit different degrees of rebound burst discharge. Shown are *in vitro* recordings and FI plots calculated at the symbols indicated above the recordings. Na^+ spike discharge was evoked by a set of 300-ms test pulses, delivered first from resting potential and then after a 500-ms hyperpolarization from −80 to −90 mV. The current protocol is shown in the lowest trace, and break marks indicate a 4.5-s recovery period between step commands. Histogram plots of the mean frequency change over the FI plots are shown at right under control conditions (black bars) and in 2 mM Cs^+ to block I_h (gray bars). Large-diameter DCN cells exhibit either a strong burst (*A*) or weak burst (*B*). By comparison, Purkinje cells (*C*) and Golgi cells (*D*) exhibit a moderate rebound discharge. I_h contributes to rebound bursts only in Purkinje cells.

delivered from a resting potential of around −55 mV to inactivate T-type channels, and the second followed a strong hyperpolarization (around −90 mV) to recover T-type channels. Note that this protocol provides the traditional test of a single hyperpolarizing pulse followed by a return to resting levels (Fig. 3; 0 pA) and tests the influence of hyperpolarizing-activated currents over a full FI plot. Strong rebound bursts were defined as ≥25 Hz mean increase in firing frequency after the hyperpolarization over the entire FI plot.

Recordings revealed that large-diameter DCN cells fell into two distinct groups at an incidence of ≈50%: strong rebound bursters (DCN-burst) and a weak-bursting class (DCN-weak burst). DCN-burst cells showed a significant increase in frequency of up to 360 Hz (144 ± 39 Hz; $n = 7$) after hyperpolarization, whereas DCN-weak bursting cells showed only a small increase in firing frequency (6 ± 3 Hz; $P < 0.05$; $n = 6$) (Fig. 3 *A* and *B*). As both of these groups discharged tonic action potentials at a rate of ≈20 Hz at rest, the rebound burst was the clearest means of separating these populations of large DCN neurons. By comparison, Purkinje cells showed a rebound burst with a mean spike frequency increase of 28 ± 4 Hz ($n = 9$) and Golgi cells 27 ± 13 Hz ($n = 5$) over the entire FI plot (Fig. 3 *C* and *D*).

A potential contributing factor to rebound discharge is the activation of hyperpolarization-activated current (I_h) (27), which could often be detected in all four cell types as a depolarizing sag during a hyperpolarizing step (Fig. 3). We thus applied 2 mM Cs^+ or in some cases ZD 7228 to block I_h and repeated the above tests. These studies established that I_h does not play a substantial role in burst generation in DCN-burst, DCN-weak burst, or Golgi neurons, with no significant difference in the mean rebound spike frequency between control and I_h blocked conditions (Fig. 3 *A*, *B*, and *D*). By comparison, ≈60% of the rebound spike frequency increase in Purkinje cells could be attributed to I_h, as suggested by an earlier report (Fig. 3*C*) (28).

Control of Rebound Discharge in Cerebellar Neurons. These data show that rebound bursts in three of four cell types is consistent with the expression of T-type calcium current, as suggested by the pattern of Ca_v3 immunolabel (Figs. 1 and 2). Our data also identify a previously unrecognized difference in the properties of large-diameter DCN cells, in which one group generates a strong rebound discharge and the other little or no rebound discharge. The non-bursting DCN cells could simply correspond to the subset of DCN cells that were negative for a given Ca_v3 channel immunolabel (Fig. 1 *G–I*). Alternatively, the inability to generate a rebound burst could reflect the relative density or kinetics of expressed Ca_v3 isoforms or a block of the LVA calcium spike by potassium channels (20, 29). To test the potential influence of potassium channels we examined the ability of these four cell classes to generate an isolated LVA calcium response.

Potassium Channel Control of LVA Calcium Spikes. We pharmacologically isolated calcium conductances by sequentially blocking inward and outward currents with 100 nM Tetrodotoxin (TTX), 2 mM Cs^+ (I_h), and a broad spectrum of potassium channels with 5 mM tetraethylammonium (TEA) and 1 mM 4-aminopyridine (4-AP) (Fig. 4 and Table 1, which is published as supporting information on the PNAS web site). We identified LVA calcium spike discharge by detecting the first abrupt change in the slope of the voltage trace after termination of the membrane hyperpolarization. We first perfused TTX and Cs^+ and found that this procedure revealed a large amplitude LVA spike in DCN-burst cells but not in weak bursting cells (Fig. 4 *A* and *B*). When TEA and 4-AP were then added, both DCN-burst and DCN-weak burst cells responded with a strong and short duration calcium spike after a preceding hyperpolarization (Fig. 4 *A* and *B*). Similarly, the bursting phenotypes displayed by Purkinje and Golgi cells were transformed by drug perfusions to a LVA spike response (Fig. 4 *C* and *D*). Note that this procedure did not prevent the activation of other calcium
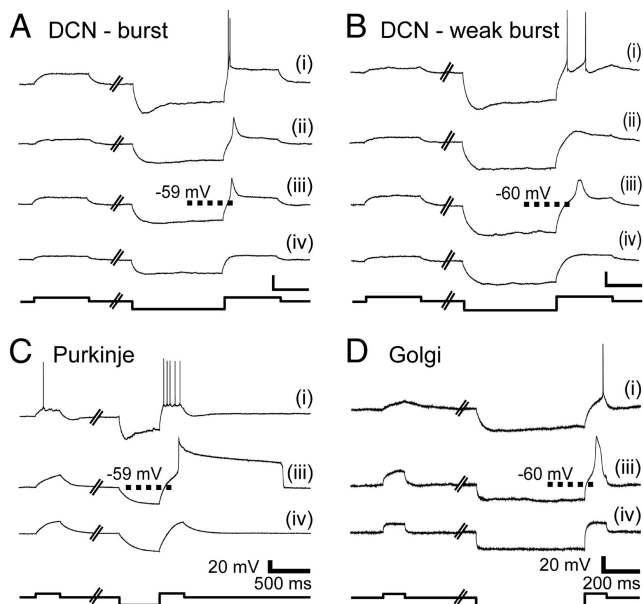
Fig. 4. Bursting and weak-bursting cerebellar cell types can exhibit isolated LVA calcium spikes. Representative recordings from the indicated cerebellar cell types are shown in normal artificial cerebrospinal fluid with sodium spike discharge intact (*i*), after addition of Tetrodotoxin (TTX) and Cs$^+$ (*ii*), or TTX, Cs$^+$, tetraethylammonium, and 4-aminopyridine (*iii*). The dashed lines denote the detected voltage threshold for the LVA calcium spike. (*iv*) Final addition of 1 mM Ni^{2+} eliminates the calcium spike response in all cases. The current injection protocol is shown below each set of recordings. (Scale bars: 200 ms and 20 mV, *A*, *B*, and *D*; 500 ms and 20 mV, *C*.)

channel types. Purkinje cells in particular extended the initial LVA calcium spike to a longer plateau depolarization indicative of high-threshold calcium channel activation under these conditions (Fig. 4*C*). In each case we verified that all remaining responses were calcium-dependent by a rapid block with 1 mM Ni^{2+} (Fig. 4) (30). LVA calcium spikes in all cells were unaffected by 5 μM nifedipine ($n = 2$–5), indicating that these responses cannot be attributed to the low-threshold L-type Ca$_v$1.3 channel. The threshold for the LVA component of the calcium spike was equivalent in both DCN cell types and consistent with T-type channels: -59 ± 2.0 mV ($n = 7$) for DCN-burst cells and -59 ± 2.4 mV ($n = 7$) for DCN-weak burst cells. Similarly, the threshold for the LVA calcium component in Purkinje cells was -57 ± 1.7 mV ($n = 6$) and in Golgi cells it was -61 ± 1.0 mV ($n = 4$) (Fig. 4 *C* and *D*).

All four cerebellar cell types examined here thus have the capacity to generate a LVA calcium spike when competing currents are blocked. This capacity was especially evident in DCN-burst and DCN-weak burst cells, where LVA and fast inactivating calcium spikes could be uncovered, suggesting a preponderance of T-type current in both cell types (Fig. 4 *A* and *D*).

DCN Cell Burst Output Correlates to the Expression of Ca$_v$3 Channel Isoforms. Our recordings establish that both DCN cell classes express Ca$_v$3 calcium channels, but do not establish whether burst properties could relate to the selective expression of one or more of the channel isoforms. A direct role for Ca$_v$3.1 channels in generating spike bursts has been established in thalamic relay cells, where a Ca$_v$3.1 knockout animal lacks burst discharge (31). We also found that expression of Ca$_v$3.1 is sufficient to support rebound burst discharge in Golgi cells, as this response was readily evoked with the expression of only Ca$_v$3.1. Purkinje cells express Ca$_v$3.1 and generate rebound bursts, but establishing the role for this channel isoform is confounded by the coexpression of Ca$_v$3.2 and Ca$_v$3.3. Rather, the clear presence or absence of specific Ca$_v$3 isoforms in
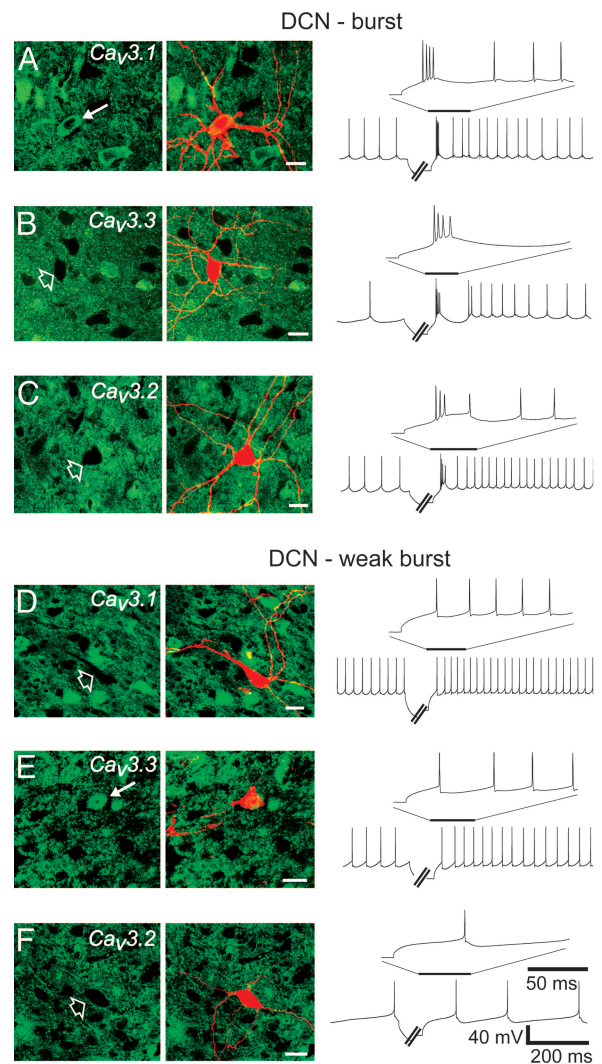

Fig. 5. DCN-burst and DCN-weak-burst neurons are selectively labeled by Ca$_v$3 channel isoforms. Shown are representative cases of DCN-burst (*A*–*C*) and DCN-weak burst cells (*D*–*F*). (*Left* and *Center*) Immunolabels for each Ca$_v$3 isoform (*Left*) and the associated neurobiotin-filled cell (*Center*). (*Right*) Recordings from each filled cell with an expanded inset of the burst. (*A*–*C*) DCN-burst neurons are positive for Ca$_v$3.1 (*A*, solid arrow; $n = 8$) but negative for Ca$_v$3.3 (*B*, $n = 5$) and Ca$_v$3.2 (*C*, $n = 5$) (open arrows). (*D*–*F*) DCN-weak bursting neurons are positive for Ca$_v$3.3 (*E*, $n = 4$) but negative for Ca$_v$3.1 (*D*, $n = 6$) and Ca$_v$3.2 (*F*, $n = 6$). Ca$_v$3 labeling was identified in a 1- to 2-μm section through the soma of the recorded cell. Neurobiotin fills are stacked sections of up to 60-μm depth superimposed on the Ca$_v$3 image. (Scale bars: 20 μm.)

individual DCN cells provided a unique opportunity to test the correlation between Ca$_v$3 immunolabel and burst phenotype.

We correlated Ca$_v$3 expression and burst phenotype by recording from DCN neurons to categorize them as burst or weak burst-capable and filled each cell with neurobiotin. Slices were then fixed and processed with one of the Ca$_v$3 antibodies and a fluorescent marker for neurobiotin, allowing us to assess the Ca$_v$3 expression pattern of individual cells. To be included in the data set, Ca$_v$3 immunolabel had to penetrate beyond the level of the filled cell soma, as judged through confocal imaging. Using this criterion we successfully compared the firing pattern of neurobiotin-filled cells with Ca$_v$3 immunolabel in 34 of 45 recorded cells. We found that DCN-burst neurons were always positive for Ca$_v$3.1 immunolabel (Fig. 5*A*; $n = 8$) but were negative for Ca$_v$3.3 (Fig. 5*B*; $n = 5$). In contrast, DCN-weak burst neurons were positive for Ca$_v$3.3 (Fig.
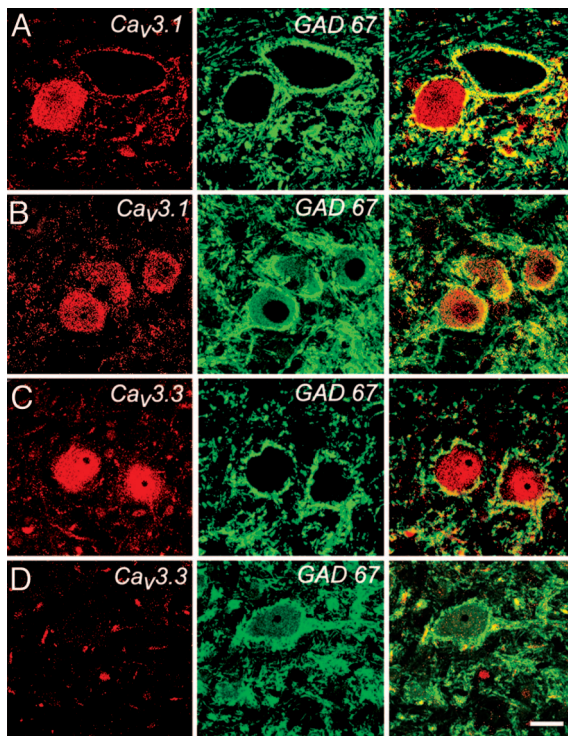
Fig. 6. Differential expression of Ca$_v$3 isoforms in GAD67-positive DCN neurons. Images of DCN cells double-labeled for GAD and either Ca$_v$3.1 or Ca$_v$3.3. Shown is immunolabel for Ca$_v$3 channels (*Left*), GAD (*Center*), and the combined images (*Right*). (*A* and *B*) DCN cells positive for Ca$_v$3.1 can be either negative (*A*) or positive (*B*) for GAD immunolabel. (*C* and *D*) Ca$_v$3.3 label is found in GAD-negative neurons (*C*) but not in GAD-positive cells (*D*). (Scale bar: 20 μm.)

5E; $n = 4$) but negative for Ca$_v$3.1 (Fig. 5D; $n = 6$). None of the DCN-burst ($n = 5$) or DCN-weak burst ($n = 6$) cells recorded here were immunoreactive for Ca$_v$3.2 (Fig. 5 C and F).

Large-diameter neurons in the DCN are known to be glutamatergic or GABAergic (21), but identifying electrophysiological signatures that can be used to discriminate between these cell classes has been difficult (23, 26). We thus examined whether bursting and weak bursting phenotypes correlated to excitatory or inhibitory neurons. We used glutamic acid decarboxylase (GAD)67 immunolabel to identify inhibitory DCN neurons and colabeled tissue sections for either Ca$_v$3.1 or Ca$_v$3.3 channels as an indicator of spike output properties. The vast majority of DCN neurons were GAD-negative, with only a few GAD-positive cells clustered together in any tissue section (Fig. 6). DCN neurons that were positive for Ca$_v$3.1 could be either GAD-positive or GAD-negative (Fig. 6 A and B), indicating that the DCN-burst cells can be either GABAergic or non-GABAergic. In contrast, all cells that were Ca$_v$3.3-positive (DCN-weak burst) were all GAD-negative (Fig. 6 C and D). We attempted to further test this finding by using cell fills and GAD colabeling.

However, GAD immunolabel could not be detected after tissue was prepared for patch recordings because of the strict fixation procedures required to sustain GAD immunogenicity. Therefore, insofar as GAD immunolabel can fully indicate the distribution of large-diameter inhibitory cells, our colabeling studies indicate that the bursting/Ca$_v$3.1 phenotype can correspond to either excitatory or inhibitory DCN neurons. The weak-bursting/Ca$_v$3.3 phenotype appears to be restricted to excitatory neurons.

Discussion

Molecular cloning studies indicate that distinct T-type calcium channel isoforms are expressed from three different genes (α_{1G}/Ca$_v$3.1, α_{1H}/Ca$_v$3.2, and α_{1I}/Ca$_v$3.3) (2–5). Precise information on the distribution of these channels and their functional roles has been lacking. Here, we combined immunocytochemical and electrophysiological assays to establish the distribution of specific Ca$_v$3 channel isoforms in cerebellar neurons and their contribution to rebound burst discharge.

Distribution of Ca$_v$3 Isoforms in Cerebellum. Expression of Ca$_v$3 isoforms has been reported in cerebellum, although the distribution and relative intensity has been variable. *In situ* hybridization consistently reveals expression of Ca$_v$3.1 mRNA in rat Purkinje cells and DCN neurons, a result that is supported by immunocytochemical localization (16, 17, 32). In contrast, *in situ* hybridization for Ca$_v$3.2 reportedly revealed no message in cerebellum, whereas Ca$_v$3.3 mRNA expression appeared primarily in granule cells (16). The present study directly compares the immunolabel distribution of all three Ca$_v$3 isoforms in cerebellum. Our labeling pattern agrees well with the reported Ca$_v$3.1 distribution, but we also find extensive labeling for Ca$_v$3.2 and Ca$_v$3.3 in select cerebellar neurons. The differences between our distribution and previous *in situ* hybridization studies could reflect the relative sensitivity of *in situ* vs. immunocytochemical labeling, different splice variants of the isoforms, or technical considerations of detection. The specificity of our Ca$_v$3 distribution pattern was directly confirmed, however, by establishing that all cell types expressing a Cav3 isoform are capable of generating a LVA calcium spike under conditions of sodium, I_h, and potassium channel blockade. The LVA spike was only revealed by a preceding membrane hyperpolarization and had a threshold for activation between -65 and -57 mV, consistent with T-type calcium channel activation. It should be noted that both low-threshold L-type and R-type calcium channels are expressed in cerebellum (33–35). However, these are expressed over a narrow developmental time frame (35), and both show activation voltages more depolarized than T-type channels (33, 36, 37). We further established that generation of the LVA calcium spike occurs in the presence of nifedipine, ruling out a significant contribution by L-type calcium channels. Therefore, our results argue that the distribution of Ca$_v$3 channel expression described here underlies the capacity to generate LVA T-type calcium currents.

Physiological Roles of Ca$_v$3 Channel Isoforms. Distinguishing the physiological roles of the three different Ca$_v$3 isoforms has been challenging given the lack of specific blockers (38). Our cytochemical data presented an opportunity to assess the potential for individual Ca$_v$3 isoforms to support rebound burst discharge in DCN neurons. The deep cerebellar nuclei are comprised of several cell types that differ in morphology, transmitter phenotype, spike patterning, and postsynaptic projections (21–23, 26). DCN neurons have been shown to express LVA calcium current (39) and exhibit a rebound burst discharge (25, 40). Bursting and weak-bursting cell types have also been reported in DCN neurons, although the bursting patterns were correlated with large-diameter compared with small-diameter neurons (26). We now report a previously unrecognized distinction between large-diameter DCN cells that exhibit either of two firing patterns and show that these patterns reflect the ability to express LVA calcium spikes under normal conditions. We were also able to relate the discharge patterns of these cells to transmitter phenotype, in that Ca$_v$3.1 expression (rebound burst output) was found in both GABAergic and non-GABAergic cells, whereas Ca$_v$3.3 expression occurs only in non-GABAergic cells.

Our data indicate that selective expression of Ca$_v$3.1 is sufficient to generate a rebound burst in both DCN-burst and Golgi cells. We have thus identified the specific calcium channel isoform involved in generating rebound bursts in this class of DCN neuron. Spike output patterns have been less studied in Golgi cells, but they have been shown to exhibit rebound discharge *in vitro* and oscillatory discharge during locomotion *in vivo* (19, 41, 42). Our work now

indicates that these properties also rely on the expression of $Ca_v3.1$ channels. LVA T-type currents in Purkinje cells have been shown to participate in the burst and interburst intervals (15). Although Purkinje cells also express $Ca_v3.1$, at this time we cannot identify its specific role given the coexpression of all three Ca_v3 isoforms.

We establish that $Ca_v3.3$ channels in DCN-weak bursting cells are prevented from generating a rebound burst by the coexpression of at least tetraethylammonium- and 4-aminopyridine-sensitive potassium channels. We cannot state explicitly that the $Ca_v3.3$ channels of DCN-weak burst cells can never support rebound burst discharge. For instance, modulation of Ca_v3 or potassium current by indirect regulatory mechanisms could unmask the potential to generate a rebound burst. We also cannot discount the possibility that the ability to generate a rebound discharge could reflect the kinetic properties or density of individual Ca_v3 isoforms. It is of interest to note that our recordings show that two other cerebellar neurons that express only $Ca_v3.2$ or $Ca_v3.3$ also do not generate a rebound discharge under normal conditions (i.e., stellate and basket cells), even though both can elicit a LVA calcium spike upon blockade of potassium channels. It has been shown that the contribution of T-type channels to LVA calcium spikes can be regulated by A-type potassium channels (20, 29). Indeed, in cerebellar stellate cells, the coexpression of $Ca_v3.2$ and $Ca_v3.3$ channels with an A-type potassium current creates a novel voltage-first spike latency relationship instead of rebound discharge (20). A study in the medial vestibular nucleus, a functional homologue of the deep cerebellar nuclei, reveals a gain control mechanism that depends on calcium-activated BK potassium channels coupled to presumed T-type channels (43). Further work will be required to resolve the full set of ionic or kinetic factors that regulate the role of Ca_v3 isoforms in generating rebound bursts.

The functional outcome of Ca_v3 expression patterns on DCN-burst or weak-burst cell classes is unknown, but it should help determine their influence on postsynaptic targets. Spike discharge in DCN cells has also been shown to determine the nature of plasticity at the Purkinje-DCN synapse (11), suggesting that the inherent differences in rebound discharge patterns seen here may selectively refine Purkinje-DCN cell synaptic efficacy. A recent theory on cerebellar function postulated timing loops critically depend on rebound bursting (14). The widespread and differential expression of Ca_v3 isoforms could then impose different roles for cerebellar neurons in this timing relationship.

Materials and Methods

Animal Care. Male Sprague–Dawley rats were used at postnatal days 14–21, and procedures were conducted according to guidelines approved by the Canadian Council for Animal Care. All chemicals were obtained from Sigma, and immunochemicals were from Vector Laboratories unless otherwise indicated.

Immunocytochemistry. Antibodies directed to the $Ca_v3.1$ calcium channel were produced by using the $Ca_v3.1$ I-II linker sequence (ELRKSLLPPLIIHTAATPMS), which corresponds to amino acids 1010–1027 (GenBank accession no. AF290212). The channel peptide was cross-linked to keyhole limpet hemocyanin before injection into rabbits, and the serum was purified for use. The epitopes used for the $Ca_v3.2$ and $Ca_v3.3$ antibody were produced by using the *Caulobactor* expression system (Invitrogen) and corresponded to amino acids 1195–1273 (GenBank accession no. AF290213) and amino acids 1013–1115 (GenBank accession no. AF290214) for the $Ca_v3.2$ and $Ca_v.3.3$ calcium channel II-III linkers, respectively. Purified proteins were injected into rabbits, and the polyclonal antibodies were purified before use.

Electrophysiology. Parasagittal tissue slices (300 μm) were prepared from cerebellum as detailed (12) and recorded at 35°C as a submerged preparation. Whole-cell recordings were obtained by using an internal solution of 130 mM K-gluconate, 0.1 mM EGTA, 10 mM Hepes, 7 mM NaCl, 0.3 mM di-Tris-creatine phosphate, 2 mM Tris-ATP, and 0.5 mM Na-GTP, pH 7.3 with KOH, supplemented with 1% neurobiotin for cell identification. Recordings were obtained by using an Axoclamp 2A amplifier (Axon Instruments, Union City, CA), and data were collected with PCLAMP 8.1 software. Junction potentials of ≈10 mV were not subtracted from recordings. Resting membrane voltage was between −45 mV and −55 mV depending on cell type and between −80 mV and −90 mV during the hyperpolarizing step. All recordings were carried out in bath-applied blockers of glutamatergic and GABAergic synaptic transmission after obtaining the initial seal. Further details are provided in *Supporting Methods*, which are published as supporting information on the PNAS web site.

1. Huguenard, J. R. (1996) *Annu. Rev. Physiol.* **58**, 329–348.
2. Perez-Reyes, E., Cribbs, L. L., Daud, A., Lacerda, A. E., Barclay, J., Williamson, M. P., Fox, M., Rees, M. & Lee, J. H. (1998) *Nature* **391**, 896–900.
3. Lee, J. H., Daud, A. N., Cribbs, L. L., Lacerda, A. E., Pereverzev, A., Klockner, U., Schneider, T. & Perez-Reyes, E. (1999) *J. Neurosci.* **19**, 1912–1921.
4. Williams, M. E., Washburn, M. S., Hans, M., Urrutia, A., Brust, P. F., Prodanovich, P., Harpold, M. M. & Stauderman, K. A. (1999) *J. Neurochem.* **72**, 791–799.
5. McRory, J. E., Santi, C. M., Hamming, K. S., Mezeyova, J., Sutton, K. G., Baillie, D. L., Stea, A. & Snutch, T. P. (2001) *J. Biol. Chem.* **276**, 3999–4011.
6. McCormick, D. A. & Huguenard, J. R. (1992) *J. Neurophysiol.* **68**, 1384–1400.
7. Jahnsen, H. & Llinas, R. (1984) *J. Physiol. (London)* **349**, 227–247.
8. Jahnsen, H. & Llinas, R. (1984) *J. Physiol. (London)* **349**, 205–226.
9. Deschenes, M., Paradis, M., Roy, J. P. & Steriade, M. (1984) *J. Neurophysiol.* **51**, 1196–1219.
10. Muri, R. & Knopfel, T. (1994) *J. Neurophysiol.* **71**, 420–428.
11. Aizenman, C. D., Manis, P. B. & Linden, D. J. (1998) *Neuron* **21**, 827–835.
12. McKay, B. E., Molineux, M. L., Mehaffey, W. H. & Turner, R. W. (2005) *J. Neurosci.* **25**, 1481–1492.
13. Telgkamp, P. & Raman, I. M. (2002) *J. Neurosci.* **22**, 8447–8457.
14. Kistler, W. M. & De Zeeuw, C. I. (2003) *Cerebellum* **2**, 44–54.
15. Swensen, A. M. & Bean, B. P. (2003) *J. Neurosci.* **23**, 9650–9663.
16. Talley, E. M., Cribbs, L. L., Lee, J. H., Daud, A., Perez-Reyes, E. & Bayliss, D. A. (1999) *J. Neurosci.* **19**, 1895–1911.
17. Craig, P. J., Beattie, R. E., Folly, E. A., Banerjee, M. D., Reeves, M. B., Priestley, J. V., Carney, S. L., Sher, E., Perez-Reyes, E. & Volsen, S. G. (1999) *Eur. J. Neurosci.* **11**, 2949–2964.
18. Midtgaard, J. (1992) *J. Physiol. (London)* **457**, 329–354.
19. Dieudonne, S. (1998) *J. Physiol. (London)* **510**, 845–866.
20. Molineux, M. L., Fernandez, F. R., Mehaffey, W. H. & Turner, R. W. (2005) *J. Neurosci.* **25**, 10863–10873.
21. Sultan, F., Konig, T., Mock, M. & Thier, P. (2002) *J. Comp. Neurol.* **452**, 311–323.
22. Chan-Palay, V. (1977) *Cerebellar Dentate Nucleus: Organization, Cytology, and Transmitters* (Springer, Berlin).
23. Sultan, F., Czubayko, U. & Thier, P. (2003) *J. Comp. Neurol.* **455**, 139–155.
24. D'Angelo, E., De Filippi, G., Rossi, P. & Taglietti, V. (1997) *J. Neurophysiol.* **78**, 1631–1642.
25. Aizenman, C. D. & Linden, D. J. (1999) *J. Neurophysiol.* **82**, 1697–1709.
26. Czubayko, U., Sultan, F., Thier, P. & Schwarz, C. (2001) *J. Neurophysiol.* **85**, 2017–2029.
27. Pape, H. C. (1996) *Annu. Rev. Physiol.* **58**, 299–327.
28. Crepel, F. & Penit-Soria, J. (1986) *J. Physiol. (London)* **372**, 1–23.
29. Pape, H. C., Budde, T., Mager, R. & Kisvarday, Z. F. (1994) *J. Physiol. (London)* **478**, 403–422.
30. Zamponi, G. W., Bourinet, E. & Snutch, T. P. (1996) *J. Membr. Biol.* **151**, 77–90.
31. Kim, D., Song, I., Keum, S., Lee, T., Jeong, M. J., Kim, S. S., McEnery, M. W. & Shin, H. S. (2001) *Neuron* **31**, 35–45.
32. Yunker, A. M. (2003) *J. Bioenerg. Biomembr.* **35**, 577–598.
33. Tottene, A., Moretti, A. & Pietrobon, D. (1996) *J. Neurosci.* **16**, 6353–6363.
34. Regan, L. J. (1991) *J. Neurosci.* **11**, 2259–2269.
35. Liljelund, P., Netzeband, J. G. & Gruol, D. L. (2000) *J. Neurosci.* **20**, 7394–7403.
36. Randall, A. D. & Tsien, R. W. (1997) *Neuropharmacology* **36**, 879–893.
37. Lipscombe, D., Helton, T. D. & Xu, W. (2004) *J. Neurophysiol.* **92**, 2633–2641.
38. Jimenez, C., Bourinet, E., Leuranguer, V., Richard, S., Snutch, T. P. & Nargeot, J. (2000) *Neuropharmacology* **39**, 1–10.
39. Gauck, V., Thomann, M., Jaeger, D. & Borst, A. (2001) *J. Neurosci.* **21**, RC158.
40. Jahnsen, H. (1986) *J. Physiol. (London)* **372**, 129–147.
41. Vos, B. P., Volny-Luraghi, A., Maex, R. & De Schutter, E. (2000) *Prog. Brain Res.* **124**, 95–106.
42. Edgley, S. A. & Lidierth, M. (1987) *J. Physiol. (London)* **392**, 315–332.
43. Smith, M. R., Nelson, A. B. & Du Lac, S. (2002) *J. Neurophysiol.* **87**, 2031–2042.